Published in IET Microwaves, Antennas & Propagation
Received on 26th September 2008
Revised on 25th August 2009
doi: 10.1049/iet-map.2008.0339

ISSN 1751-8725

Investigation of on-body Bluetooth transmission

M. Ur Rehman[1] *Y. Gao*[1] *Z. Wang*[1] *J. Zhang*[1] *Y. Alfadhl*[1] *X. Chen*[1] *C.G. Parini*[1] *Z. Ying*[2] *T. Bolin*[2]

[1]*Department of Electronic Engineering, Queen Mary University of London, London, UK*
[2]*Sony Ericsson Mobile Communications AB, Lund, Sweden*
E-mail: masood.rehman@elec.qmul.ac.uk

Abstract: The development of communication devices, especially cellular phones has necessitated the advances of several portable and wearable technologies, such as Bluetooth headsets within wireless body area networks (WBAN). Such wearable devices use the human body as a communication channel; hence, a comprehensive understanding of the transmission mechanism between such devices is vital. This study presents an investigative study to characterise the electromagnetic transmission between a body-mounted Bluetooth headset antenna and a mobile phone handset antenna. Commercially used antennas have been used to study various factors affecting on-body communication links including handset-to-body separation and presence of blocking objects. A thorough numerical modelling, supported by the measurements, has been carried out to demonstrate the importance of surface waves in the on-body Bluetooth transmission.

1 Introduction

The evolution of portable mobile phones, personal digital assistants (PDAs), personal navigation devices (PNDs) and laptops has brought a revolution in the field of wireless communications. This rapid growth of research and development has been promoted by the wider approach, mobility and ease of use provided by these devices. The human body is an integral part of the wireless body area network (WBAN) applications and therefore electromagnetic interaction between the human body and antennas has been studied for many years [1, 2]. It is now well established that the close proximity of the human body degrades the performance of the antennas significantly [1–9]. The very lossy nature of human tissues causes high level of losses over the communication spectrum. The resulting phenomena effects on the antenna performance by introducing distortion in the radiation pattern, reduction in radiation efficiency and detuning in antenna input impedance [5–9].

In principle, the human body can be used as a communication channel for different devices that are located within a close proximity as well as body-worn devices. A typical scenario may involve a Bluetooth enabled body-worn mobile handset and a Bluetooth headset forming a similar wireless communication link. Characterisation of such on-body channel has attracted the interest of many researchers around the world. Various characterisation criteria have been taken into account to evaluate this communication channel including path gain, radiation pattern, gain and efficiency of different antennas [4, 7–9]. The influences of varying the body postures and the different antenna types on the on-body communication channel, as well as the on-body channel path gain for a moving human body have also been studied [7, 8].

The on-body wireless communication link involves two mediums for the transfer of signals, the human body and the air. It was noticed that when there is no line-of-sight and reflecting objects, the transfer of electromagnetic energy between two body-mounted antennas takes place mostly in the form of surface waves [8–11]. These waves are generated in, and guided by the air–body interface. Studies have also shown that these surface waves may play an important role in ultra-wide band (UWB) communications [6]. However, most of these studies were only concerned with the models

of a small part of the human body with shorter on-body channels and generic antennas. In practical scenarios, on-body communication link requires a better insight into the on-body radio wave propagation including effects of antenna orientations and presence of blocking objects so that possible measures can be taken to improve the link budget. Therefore it would be interesting to examine the role of these surface waves in practically used larger on-body Bluetooth links involving a complete human body model.

This paper presents an investigation into the on-body Bluetooth transmission mechanism using a simplified homogenous human body model in simulations and measurements. Commercially available planar inverted F antenna (PIFA) on a mobile phone handset and a meander line monopole on a headset have been used in this study, provided by Sony Ericsson. An in-depth study of the on-body transmission mechanism was carried out by exploring different orientations of the handset antenna, varying separations between the body and the handset antenna and the presence of blocking objects in the communication path.

The content of this paper is organised as follows: In Section 2, both headset and handset antennas are characterised in simulations and measurements. In Section 3, the Bluetooth link budget between the PIFA in mobile handset and the meander line monopole in the Bluetooth headset at 2440 MHz is studied in the absence of the human body as well as in its presence. Effects of change in the orientation of the handset PIFA on this on-body link are also analysed. In Section 4, the on-body transmission mechanism for the Bluetooth link is investigated and importance of the surface waves is highlighted through electric field distributions and received signal strengths. Effects of the separation between the body and the handset antenna, presence of a horizontal metal barrier and separation between the barrier and the body are also studied to further establish the role of the surface waves. Finally, conclusions are drawn in Section 5.

2 Headset and handset antennas

2.1 Headset antenna

The headset antenna used in this study is a meander line monopole. The antenna is implemented in one of Sony Ericsson's Bluetooth headsets mounted at one end of the PCB, as illustrated in Fig. 1*a*. Simulations were carried out in CST Microwave Studio® using a discrete feeding port. Figs. 1*b* and *c* show the antenna performance in free space. It can be seen that the antenna has a very wide coverage over the Bluetooth band. It has a −10 dB bandwidth of 592 MHz, ranging from 2142 to 2734 MHz. The 3-D radiation pattern indicates a typical donut shape with a maximum gain value of 2.7 dBi. It is verified by measuring the 2-D patterns on the $x-y$ and $y-z$ planes in Antenna Measurement Lab at Queen Mary University of London. The 2-D patterns are shown in Fig. 2. The measurements agree well with the simulated results.

2.2 Handset antenna

A mobile handset (one of Sony Ericsson's mobile phone model K750i) with a PIFA as the radiating element has been modelled in this study. The PIFA is mounted on a ground plane of 100 mm × 40 mm and fed by a coaxial port as shown in Fig. 3*a*. The antenna itself is not visible as it is covered by the mobile casing. Figs. 3*b* and *c* show the antenna performance in terms of simulated and measured return losses, and simulated 3-D radiation pattern. It is noted that the measured resonance is shifted slightly upward because of the fact that the antenna is surrounded by other components including LCD, camera and casing that are not included in the model (Fig. 2a). Nevertheless, the measured and simulated return losses both cover the −10 dB bandwidth of 206 MHz in the required frequencies,

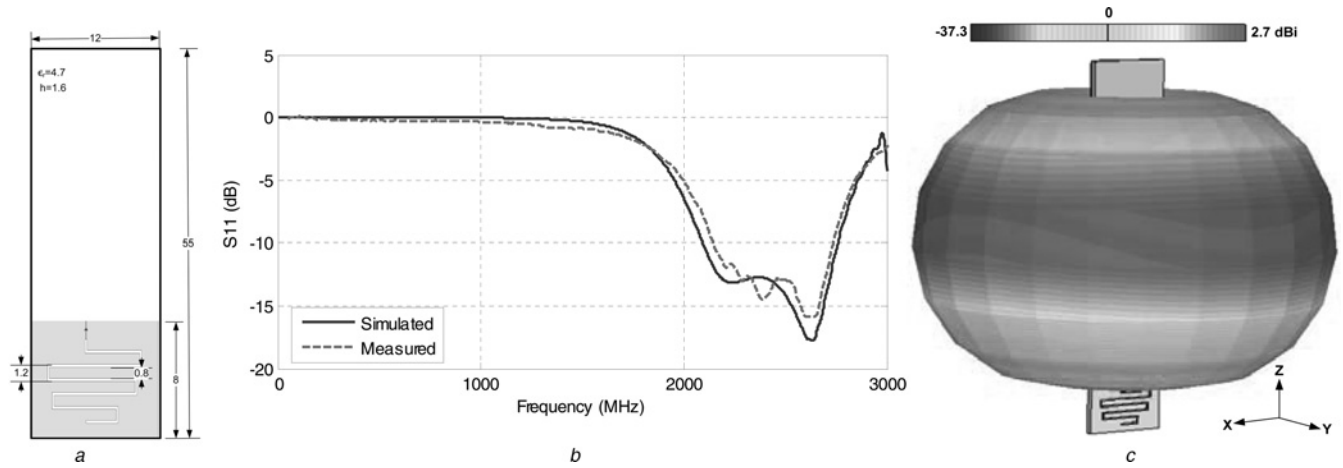

Figure 1 *Headset meander line monopole antenna geometry and performance for the Bluetooth operation*

a Antenna geometry
b Simulated and measured return loss curves
c Simulated 3-D radiation pattern

doi: 10.1049/iet-map.2008.0339

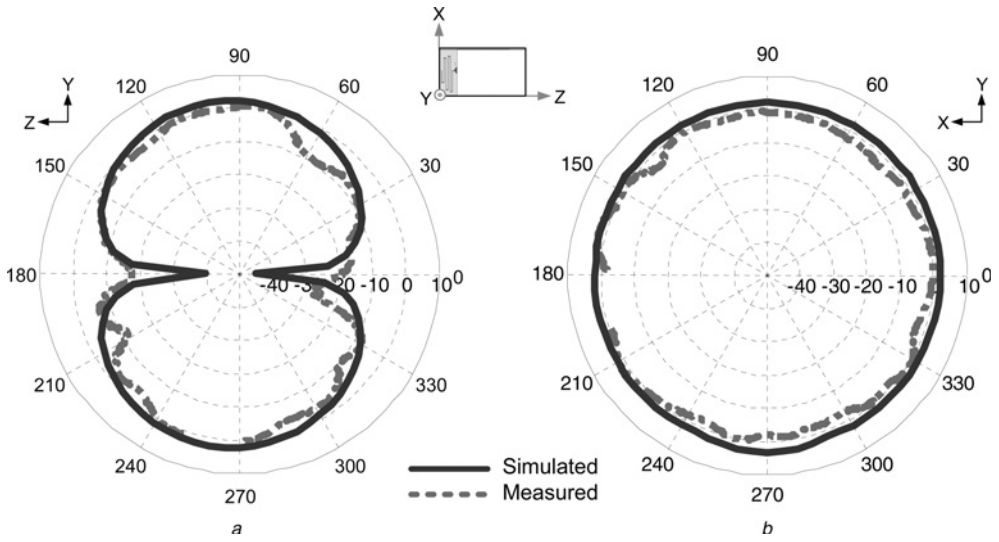

Figure 2 *Comparison of simulated (blue) and measured (red) 2-D radiation patterns of the Bluetooth headset antenna at 2440 MHz*

a *y–z* plane
b *x–y* plane

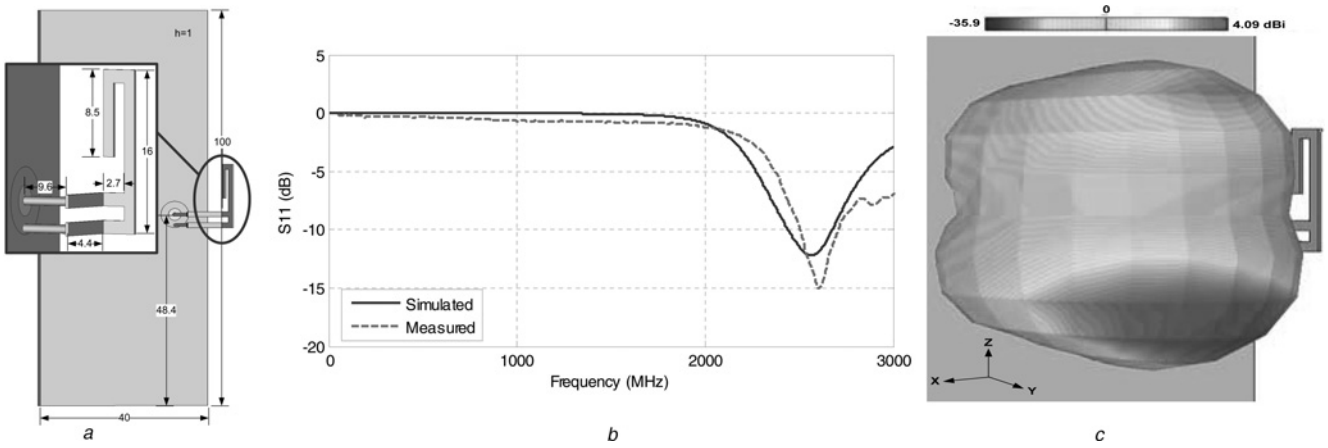

Figure 3 *Handset PIFA antenna geometry and performance for the Bluetooth operation*

a Antenna geometry
b Simulated and measured return loss curves
c Simulated 3-D radiation pattern

sufficient for the Bluetooth applications. Fig. 3*c* shows a complicated 3-D radiation pattern with a maximum gain of 4.09 dBi in $\phi = 90^\circ$, $\theta = 135^\circ$ direction. The comparison of simulated and measured 2-D radiation patterns on the x–y and y–z planes is illustrated in Fig. 4, where a good agreement can be observed.

3 On-body Bluetooth link

3.1 Human body modelling

A single layer human body model has been developed using the CST Microwave Studio®, which is based on the finite integration technique (FIT) [12]. Owing to the complexity of the human body composition, the tissue properties have been averaged out by estimating weight of the main tissue contents. The homogeneous human model was approximated to include 10% skin, 30% fat, 40% muscle and 20% bone, which leads to an averaged relative permittivity of 28.16 and conductivity of 1.14 S/m at 2440 MHz [13].

The high level discretisation of the whole-body model represents an average built human with a height of 1740 mm. An adaptive meshing scheme has been implemented where finer cell sizes have been used around the vital parts of the body. This scheme reduces the required number of cell volumes (voxels) in the computational domain significantly, hence the computation and time requirements. The perfectly matched layer (PML) absorbing boundary conditions are used [14], with a maximum mesh

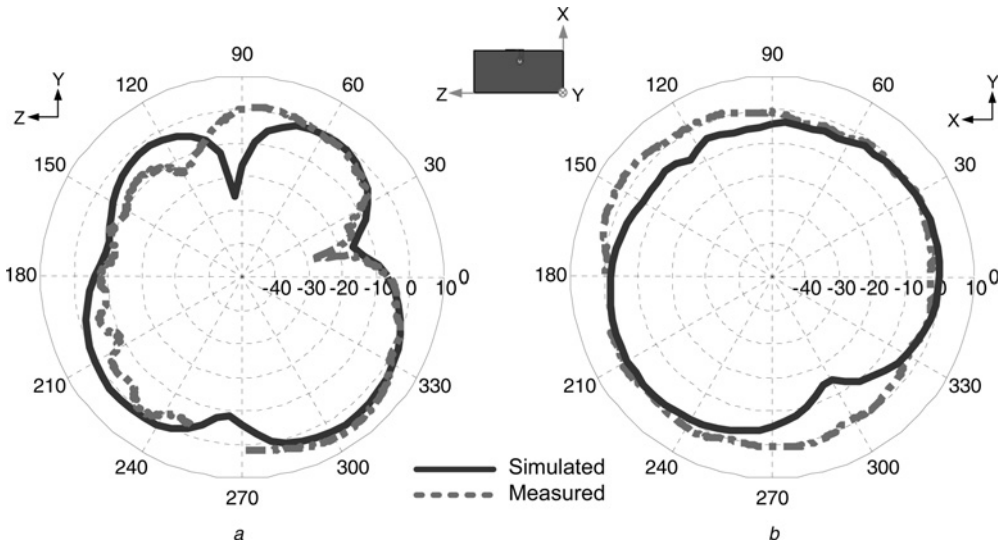

Figure 4 *Comparison of simulated (dark grey) and measured (light grey) 2-D radiation patterns of the PIFA handset antenna at 2440 MHz*

a *y–z* plane
b *x–y* plane

cell size of 10 mm near the boundaries of the computational domain and a minimum mesh cell size of 0.08 mm at the edges of the solids in the computational domain. The headset antenna was placed 10 mm away from the head at approximate location of the ear in order to incorporate the clearance for the cover assembly. The handset antenna was placed on right side of the body model at waist realising a typical body-worn position, with the same separation of 10 mm from the body to add the cover assembly clearance.

In this study, the main interest lies in the investigation of the surface wave behaviour in on-body communication links. Earlier publications have reported that in such studies, simple human body models could also deliver accurate results [5]. To confirm this, a simple homogeneous model of a volunteer was also designed. This simple body model was 1700 mm high and a thickness of the torso of 120 mm. The radius of the head was set to 86 mm. Since the major area of concern is the upper part of the body (from thighs to head) between the handset and the headset antennas, the lower part of the model (knees to feet) was not included for the sake of computational efficiency. This approach reduced the effective length of the body model to 1100 mm. The location of the headset and the handset antennas were kept the same as above with 10 mm separation from the body surface. The structure of the two models is illustrated in Fig. 5.

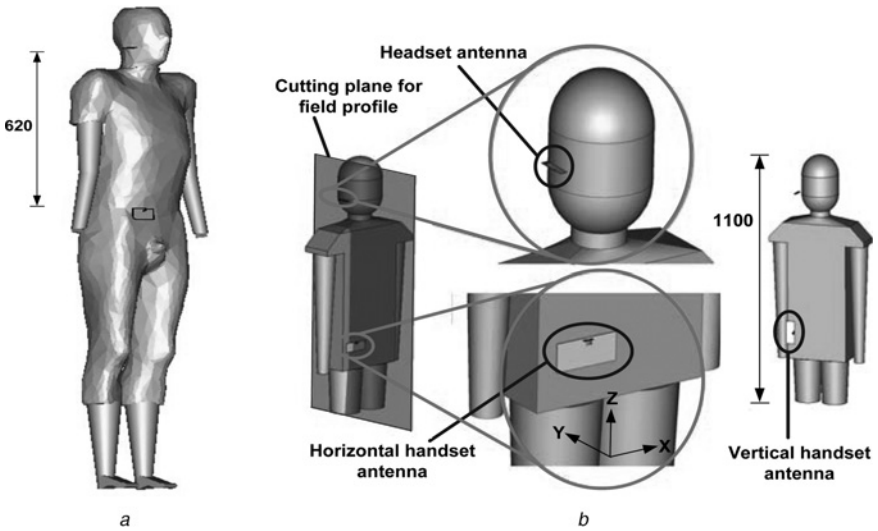

Figure 5 *Numerical models of the human body and on-body test configurations*

a Realistic high resolution whole-body model with horizontal handset
b Simple thigh-to-head model with two handset antenna orientations and cross-section plane for observation of electric field distribution (all lengths are in mm)

doi: 10.1049/iet-map.2008.0339

The electric field distributions on the body surface were investigated on the cross-section plane through the headset as shown in Fig. 5*b* and were then compared for the two models. The fields were normalised to the value at the feeding point of the handset antenna as presented in Fig. 6. From these results, it is obvious that the two models support a similar field pattern. In both cases, the field strength at the headset antenna is in the order of −18 dB. It is also evident from Fig. 6*a* that the lower part of the body is not a contributor to the Bluetooth on-body link between the handset and the headset antenna. These factors lead to the choice of a simpler model for further investigations. The close agreement between the simulated and measured values of path gain observed in the next section further increases the level of confidence in the use of this simple model whose benefits in terms of computational resources are clear.

3.2 Simulations and measurements

Two orientations of the handset antenna, horizontal and vertical, have been considered. In the horizontal arrangement, the antenna ground plane is parallel to the body, longitudinal in x-axis with the PIFA at the top of the ground plane. In vertical arrangement, the antenna is rotated 90°, now having the ground plane longitudinal in z-axis with the PIFA on the left as described in Fig. 5*b*. The vertical distance between the headset and the handset antennas is 620 mm.

The Bluetooth link is characterised in terms of average path gain ($|S21|$). The simulated results were confirmed by the measurements using Agilent HP8720ES Vector Network Analyser. The headset and handset antennas were worn by the volunteer of almost the same body structure and arranged in the same configurations as was modelled.

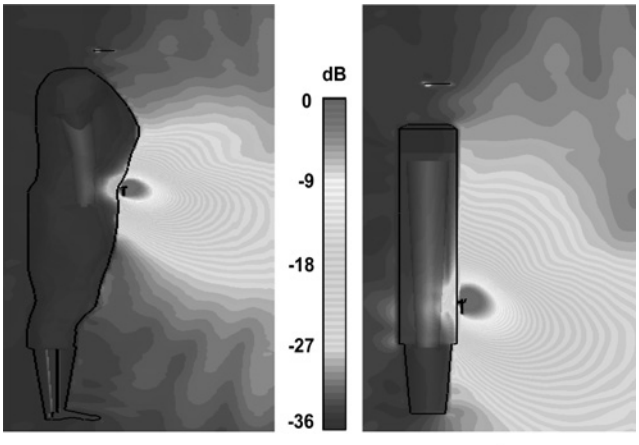

Figure 6 *Comparison of normalised electric field distributions and on-body surface waves on realistic body model and simple body model for horizontally oriented handset*

a Realistic whole-body model (cross-section view)
b Simple thigh-to-head model (cross-section view)

The two antennas were fed by low-loss coaxial cables of 5 m length. The coupling between two feed cables was measured separately and a loss variation of 0.5 dB (maximum) was found on-body. The handset and headset antenna prototypes used in the measurements are shown in Fig. 7a while the on-body measurement set-up in an anechoic chamber is illustrated in Fig. 7*b*.

Initially, the Bluetooth link was studied in the absence of the human body. In this scenario, the handset PIFA antenna and the headset meander line monopole antenna were placed at the same locations where they would be in the presence of the human body. Therefore the test set-up is essentially the same as described in Fig. 5, but without the presence of the human body model. It was noticed that the direct link between the handset and the headset antenna was −36.8 dB in simulation and −36.5 dB in measurement at 2440 MHz. Placing the handset antenna in vertical orientation has caused some drop in path gain and the simulated and measured values of the average path gain appeared to be −38.3 and −37.2 dB, respectively. This decrease in the path gain can be easily understood as the directivity of the vertical oriented handset antenna is dropped in the upward direction (z-axis) as shown in the radiation pattern in Fig. 3*c*. In general, the simulated and measured results represent a close agreement to each other.

The Bluetooth link has also been investigated for on-body transmission with body-worn handset and headset antennas. Both horizontal and vertical placements of the handset antenna were taken into account. The simulated and measured average path gain between the body-worn, horizontally placed handset and the headset were found to be −51.6 and −52.0 dB, respectively at 2440 MHz. On the other hand, path gain for the body-worn vertically placed handset configuration was found to be −49.1 dB in simulation whereas −47.6 dB in measurement. Table 1 summarises the simulated and measured results of the

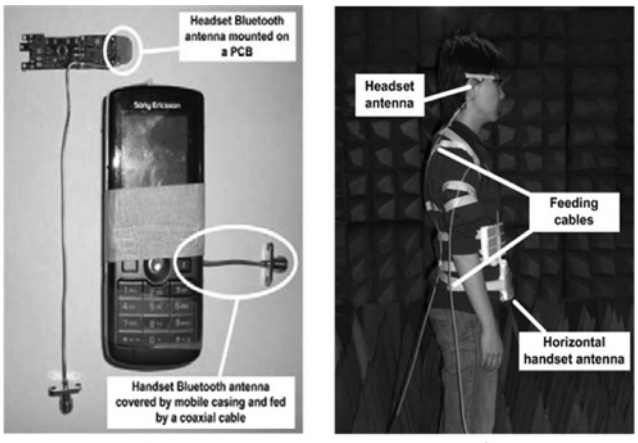

Figure 7 *Antenna prototypes and on-body test set-up used for the measurements*

a Antenna prototypes
b On-body measurement set-up

Table 1 Simulated and measured values of the average path gain (|S21|) for different test configurations, with different handset antenna orientations and with and without human body

Test set-up	Average path gain (|S21|) dB	
	Simulated	Measured
horizontal handset, without body	−36.8	−36.5
horizontal handset on-body	−51.6	−52.0
vertical handset, without body	−38.3	−37.2
vertical handset on-body	−49.1	−47.6

average path gains between the handset and the headset antennas in different test configurations.

It is not surprising that the path gain drops substantially in the presence of the human body, which blocks the line-of-sight between the headset and handset antennas. However, the decrease in link differs with the change in handset orientation: 14.8 dB (simulation) or 15.5 dB (measurement) in case of horizontally placed handset and 10.8 dB (simulation) or 10.4 dB (measurement) in case of vertically placed handset. This apparent difference caused by the orientation of the handset antenna will be explained when the role of the surface waves is addressed in the next section.

The simulated path gains have shown a good overall agreement to the measured values. A maximum difference of 1.5 dB occurred in the case of vertical handset on-body. Possible reasons for this small error lie in the small differences between the computer model and the experiment, such as the shape of the body, tissue properties, presence of clothes and feeding cables. However, this close agreement between the two values validates the computer models and serves as a benchmark for further study of on-body communication link. It also justifies the choice of a simple homogeneous model to study the on-body Bluetooth transmission mechanism in the following section.

4 Role of surface waves

The path gain values obtained in the previous section are useful in designing the Bluetooth enabled handsets and headsets. However, further insights into the electromagnetic wave propagation are required in order to devise means to improve this communication link. The electromagnetic energy travels from a transmitting antenna to a receiving antenna placed at short distances above a lossy conductor such as the human body in two ways; air (space) waves and the surface waves [15]. The induced currents in the surface of the lossy conductor produce a downward tilt and diffract the wave-front of the radio signal. It results in the formation of the surface waves on

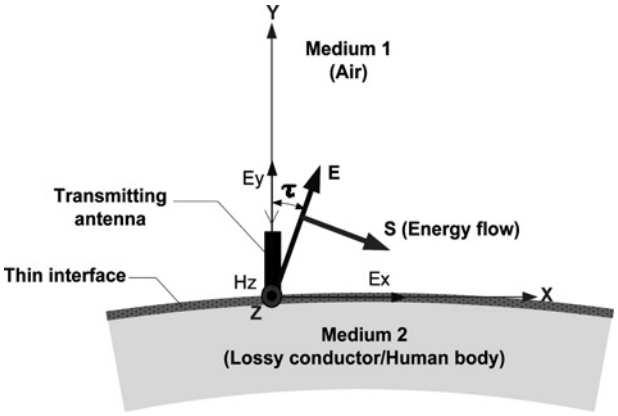

Figure 8 *Generation of surface waves on the interface of air and lossy conductor because of downward tilt of the wave-front*

the interface of the two mediums that follows the curvature of the surface [16] as depicted in Fig. 8. In the absence of line-of-sight, these surface waves play an important role to establish an efficient wireless communication link. Attenuation of these surface waves depends considerably on the electric properties of the surface [17, 18].

In this section, distribution of electric field magnitude and received signal strength is employed to investigate the role of the surface waves in the on-body Bluetooth link. The received signal strength is calculated from the electric field on the human body surface along the path between the two antennas. The electric field distribution is plotted on the cross-section plane normal to the *x*-axis cutting through the headset antenna as illustrated in Fig. 5*b* and on the front surface of the body, respectively. The electric field is normalised to the value at the feeding point of the handset PIFA antenna. Different scenarios including changing handset antenna orientation, varying handset–body separation and presence of blocking object in the transmission path at varying gaps from the human body are considered to highlight the importance of the surface waves.

4.1 Effects of handset antenna orientation

The two orientations of the mobile handset PIFA antenna; horizontal and vertical were re-investigated to study the surface wave's behaviour. Figs. 9 and 10 show distributions of normalised electric field magnitude, viewed on the cross-section plane through the headset and the front surface of the body for horizontal and vertical orientation, respectively. It is evident from the electric field distributions in Figs. 9*a* and 10*a* that diffraction of the air waves along the surface of the human body results in the generation of the surface waves. These surface waves are guided by the air–body interface and creeps towards the headset antenna. These surface waves reach almost all parts of the body but their decay is rapid due to high losses of the human body tissues as illustrated in Fig. 9*b*. Although

doi: 10.1049/iet-map.2008.0339

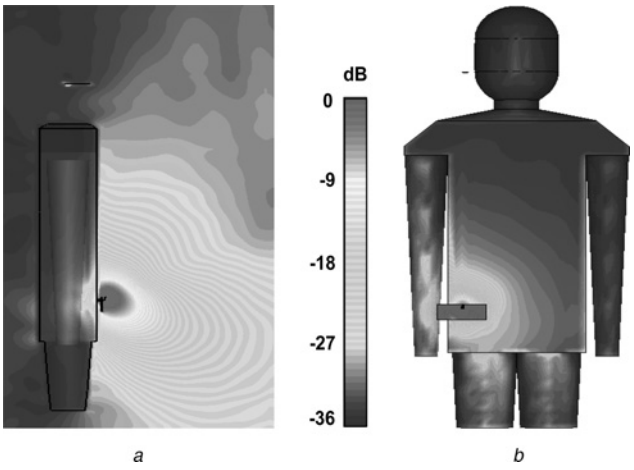

Figure 9 *Normalised electric field distribution and on-body surface waves for horizontally oriented handset*

a Cross-section plane view
b Front view

the air waves seem much stronger, their direction of propagation is away from the body because of reflections and hence, little contribution can be noted at the headset.

The electric field distribution for the vertical oriented handset in Fig. 10 depicts much stronger surface waves as compared to the horizontal oriented handset. It is due to the fact that vertical polarised signal generated by the vertical placement of the handset antenna results in the electric field perpendicular to the human body surface. It minimises the contact of the electric field with the human body reducing the energy absorption in the lossy tissues. On the other hand, electric field is parallel to the human body surface when the radio signal is in horizontal polarisation. A constant contact with the human body surface of such wave causes it to attenuate more rapidly as evident from Fig. 9. Therefore the vertical orientation of

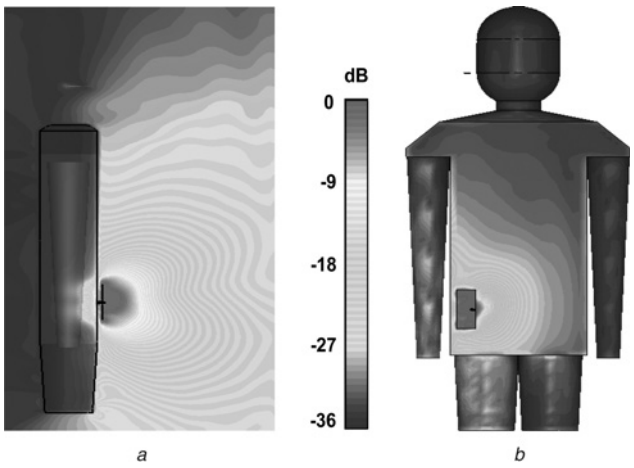

Figure 10 *Normalised electric field distribution and on-body surface waves for vertically oriented handset*

a Cross-section plane view
b Front view

the handset antenna forms a stronger on-body link with the headset antenna than the one observed for horizontal placement of the handset. The path gains for the two orientations given in Table 1 further confirm it with higher values for the vertically placed handset than that with a horizontally placed handset.

The received signal strength on the body surface in Figs. 9*b* and 10*b* is used to obtain a more insight of the surface wave behaviour in on-body transmission mechanism. The received signal values were plotted as a function of distance from the handset antenna towards the headset antenna. The origin of the three axes is located on the right side of the body, above the handset antenna. The starting point in the vertical direction (the origin of *z*-axis) for all the plots were chosen 200 mm away from the handset antenna to avoid the antenna near field region.

Fig. 11 illustrates the received signal strength along the width of the body surface (from right to left: 20–280 mm) for horizontally placed handset antenna whereas Fig. 12 describes the received signal strength for vertical orientation of the handset antenna in the same fashion. The curves on two extremes are excluded to avoid the diffraction effects on the edges. From Fig. 12 (vertically oriented handset antenna), it is obvious that there exists a nearly 'flat roof' in the region from 300 to 500 mm (from chest to shoulder) along the body surface (in the *z*-axis direction), indicating a much slower decrease in the received signal strength and hence the surface waves. On the other hand, this 'flat roof' has sharper slope with the handset antenna placed in horizontal orientation in Fig. 11, which illustrates more rapid decay of the surface waves. It further confirms that the surface wave component of the vertically polarised signal undergoes less attenuation and hence results in a

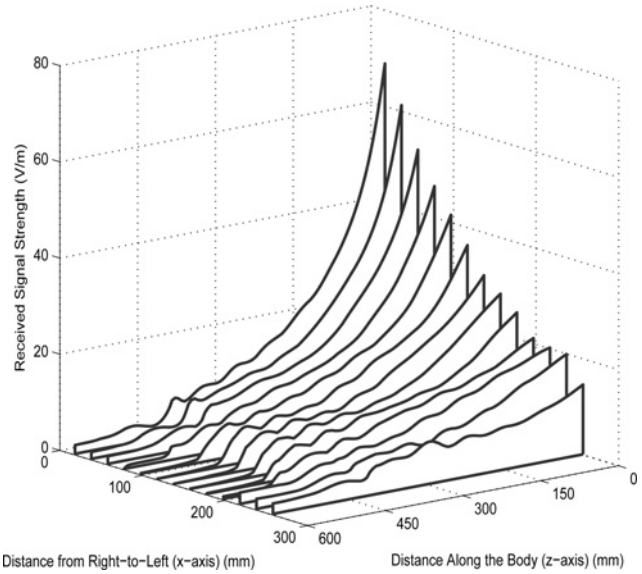

Figure 11 *Received signal strength on the path along the body surface between the horizontal handset and the headset antennas, corresponding to Fig. 9b*

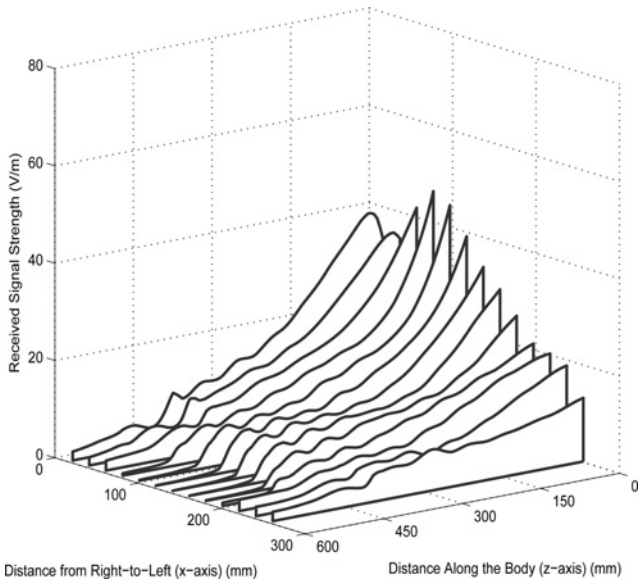

Figure 12 *Received signal strength on the path along the body surface between the vertical handset and the headset antennas, corresponding to Fig. 10b*

much stronger communication link. This, along with the field distributions shown in Figs. 9 and 10 confirms that the surface waves have a more dominant role than the air waves in the Bluetooth on-body link.

4.2 Effects of handset and body separation

The excitation condition of the on-body surface waves has been examined by analysing the effects of varying separations between the human body and the handset antenna on the Bluetooth link. The horizontally oriented handset antenna was used to investigate the worst-case scenarios. The path gain and received signal strength have been studied for handset–body separations of 10, 20 and 30 mm. Table 2 presents the path gain values obtained via simulations for the three set-ups. It is evident from these results that increasing the gap between the antenna and the human body deteriorates the on-body Bluetooth communication link.

The received signal strength on the path between the two antennas on the body surface is plotted in Fig. 13 as a function of separations between the body and the handset

Table 2 Simulated values of the average path gain (|*S*21|) for different handset–body separations with horizontally placed handset

Handset–Body separation (*d*), mm	Average path gain (|*S*21|), dB
10	−51.6
20	−52.5
30	−53.3

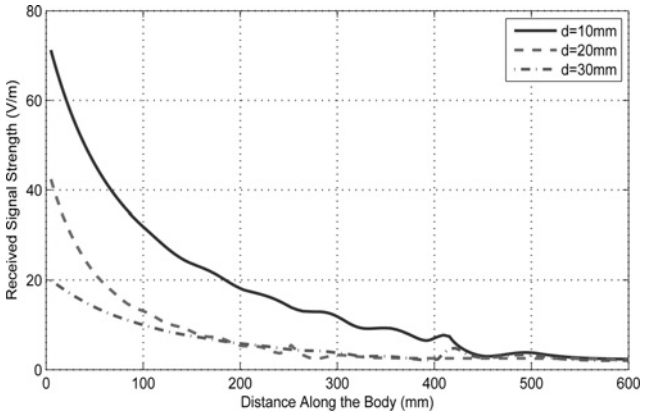

Figure 13 *Received signal strength along the body surface for different separations of horizontal handset and body*

antenna. The degradation of the Bluetooth link at 20 mm gap is apparent from the signal strength values as the surface waves are weakened because of a reduced coupling to the surface of the human body. Increase in antenna–body separation to 30 mm further reduces the strength of the surface wave component that causes the path gain to drop to −53.3 dB. These results further confirm that the surface waves are a major factor in this communication link as compared to the air waves and the 10 mm separation is the optimal position for the horizontally placed handset to excite the surface waves.

4.3 Effects of blockade by surrounding objects

Identification of the dominant transmission channel in this on-body communication link is of particular interest. It is helpful to the antenna designers to come up with designs that support the dominant medium of transmission, increasing efficiency and reliability of the communication channel. The dominant transmission medium is further determined by blocking the direct path between the handset and the headset antennas and investigating the subsequent effects on the link budget. The direct path between the two antennas was blocked using a metal barrier. The barrier has had dimensions of 458 mm × 261 mm × 20 mm and was located at a height of 140 mm from the horizontally placed handset antenna as shown in Fig. 14. Variation in the path gain values and behaviour of the surface waves because of the presence of the barrier was studied for varying barrier–body gaps. Three separating distances between the body and the barrier, that is 0, 20 and 60 mm have been considered. Table 3 gives an account of the path gain values obtained from the simulated configurations.

It can be seen that the path gain drops dramatically to −70.4 dB when the separation between the barrier and the body is set to 0 mm. Increasing the body–barrier separation shows a tendency to improve the on-body Bluetooth link. With 20 mm separation, path gain is enhanced to −58.2 dB while this value reaches to −50.2 dB with a separation of 60 mm between the body and the barrier.

doi: 10.1049/iet-map.2008.0339

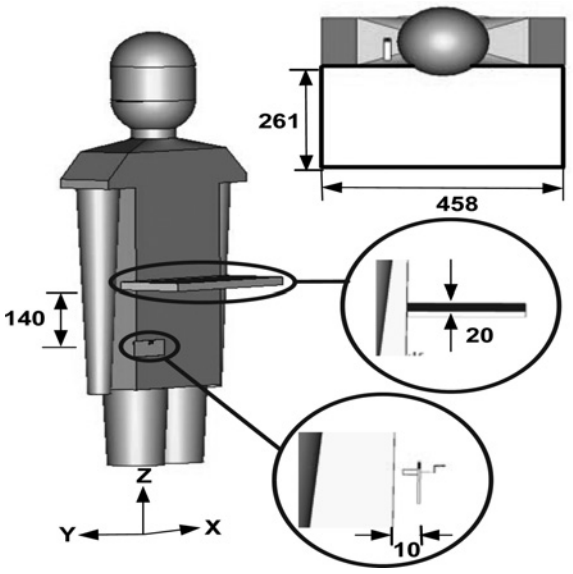

Figure 14 *On-body test configuration with horizontal handset and horizontal barrier (all lengths are in mm)*

Table 3 Simulated average path gain (|*S*21|) for surface waves' blocking effects using horizontally oriented handset

Barrier–Body separation (*d*), mm	Average path gain (|*S*21|), dB
0	−70.4
20	−58.2
60	−50.2

Fig. 15 illustrates the normalised electric field distributions in the presence of the barrier. The link is worst when there is no gap between the body and the barrier. Although a few surface waves could creep through the gap at the arms, the barrier blocks most of the air waves and the surface waves as described in Fig. 15*a* It also shows that the human body is not a good medium for communication link as little electromagnetic energy is passing through the body. Increasing the barrier–body separation to 20 mm improves the path gain because of generation and propagation of the surface waves as shown in Fig. 15*b*. In this configuration, the surface waves are the dominant medium as the air waves are still blocked.

The electric field distribution for 60 mm separation is shown in Fig. 15*c*. The link shows greater enhancement for this separation as path gain becomes −50.2 dB, 1.4 dB more than that achieved with no blocking. It can be seen that much stronger surface waves can reach the top part of the body in this case as the barrier blocks the air waves. Reflections from the barrier and diffraction at the edge of the barrier also contribute to strengthen the surface waves. Moreover, a separation of 60 mm is almost equal to the half wavelength (wavelength is 122.95 mm at 2440 MHz) whereas 20 mm is less than the quarter wavelength. The surface wave needs at least half wavelength space to pass through efficiently. Therefore the link is improved at 60 mm separation as compared to the configurations with narrower gaps. These results confirm that the surface waves creeping on the air–body interface from the handset to the headset antenna are the dominant source of energy transfer in this on-body Bluetooth transmission channel.

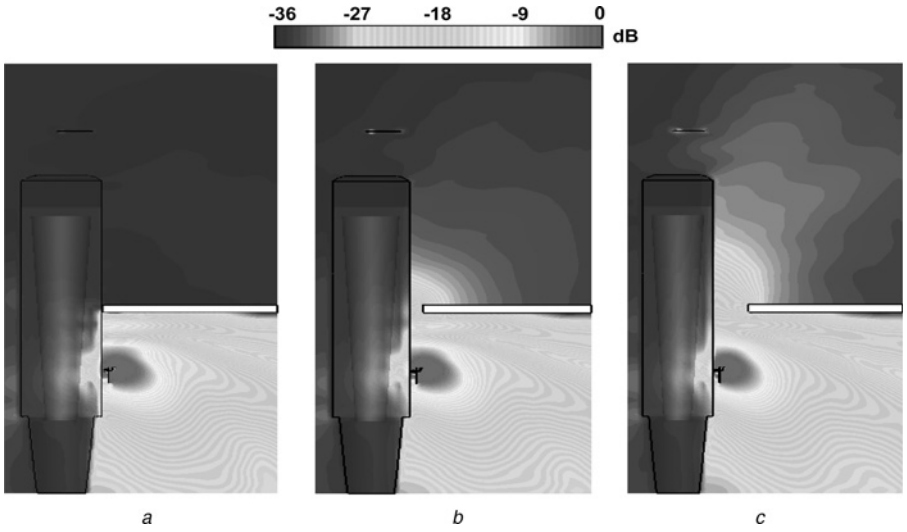

Figure 15 *Normalised electric field distribution and on-body surface waves for horizontal handset observed on the cross-section plane with barrier at different separations (d) from the body surface*

a $d = 0$ mm
b $d = 20$ mm
c $d = 60$ mm

5 Conclusions

The on-body Bluetooth link between a mobile handset and a Bluetooth headset has been analysed and verified using computer simulations and measurements. The results have shown that the human body causes a loss of about 10–15 dB in the Bluetooth path gain. This is attributed to the blocking of line-of-sight between the handset and the headset antennas. It was also evident that the surface waves play an important role in the on-body Bluetooth transmission channel. For the handset antenna, the vertical orientation has shown much stronger link as a result of the less rapid decay of the surface waves as compared to the horizontal orientation. It was also shown that increasing separations between the handset antenna and the human body has an effect on the on-body Bluetooth link because of the reduction in the surface wave excitation. It was deduced that the surface waves extend to at least half wavelength away from the human body and blocking objects located nearer than that can cause the on-body link to degrade because of blockage of the surface waves.

6 Acknowledgment

The authors would like to thank Sony Ericsson Mobile Communications for their support of this study.

7 References

[1] JENSON M.A., RAHMAT-SAMII Y.: 'EM interaction of handset antennas and human in personal communications', *IEEE Proc. Antennas Propag.*, 1995, **83**, (1), pp. 7–17

[2] OKONIEWSKI M., STUCHLY M.A.: 'A study of the handset antenna and human body interaction', *IEEE Trans. Microw. Theory Tech.*, 1996, **44**, (10), pp. 1855–1864

[3] WANG Z., CHEN X., PARINI C.G.: 'Effects of the ground and the human body on the performance of a handset antenna', *IEE Proc. Microw. Antenna Propag.*, 2004, **151**, (2), pp. 131–134

[4] RYCKAERT J., DE DONCKER P., MEYS R., DE LE HOYE A., DONNAY S.: 'Channel model for wireless communication around human body', *IET Electron. Lett.*, 2004, **40**, (9), pp. 543–544

[5] HALL P.S., HAO Y. (ED.): 'Antennas and propagation for body-centric wireless networks' (Artech House Inc., London, 2006)

[6] CHEN Z.N., CAI A., SEE T.S.P., QING X., CHIA M.Y.W.: 'Small planar UWB antennas in proximity of the human head', *IEEE Trans. Microw. Theory Tech.*, 2006, **54**, (4), pp. 1846–1857

[7] GALLO M., HALL P.S., BOZZETTI M.: 'Simulation and measurement of body dynamics for on-body channel characterization'. IET Proc. Seminar on Antennas and Propagation for Body-Centric Wireless Communications, 2007, pp. 71–74

[8] CONWAY G.A., SCANLON W.G.: 'Low-profile patch antennas for over-body-surface communication at 2.45 GHz'. Proc. IEEE Int. Workshop on Antenna Technology (IWAT), 2007, pp. 416–419

[9] HALL P.S., HAO Y., NECHAYEV Y.I., *ET AL.*: 'Antennas and propagation for on-body communication systems', *IEEE Antennas Propag. Mag.*, 2007, **49**, (3), pp. 41–58

[10] FUJII K., TAKAHASHI M., ITO K., *ET AL.*: 'Study on the transmission mechanism for wearable device using the human body as a transmission channel', *IEICE Trans. Commun.*, 2005, **E88-B**, (6), pp. 2401–2409

[11] UR REHMAN M., GAO Y., CHEN X., *ETAL.*: 'On-body bluetooth link budget: effects of surrounding objects and role of surface waves'. Proc. Loughborough Antennas and Propagation Conf. (LAPC), 2008

[12] CST Microwave Studio® 2009 User Manual

[13] GABRIEL C.: 'Compilation of the dielectric properties of body tissues at RF and microwave frequencies'. Brooks Air Force Technical Report, 1996, AL/OE-TR-1996-0037. Available at FCC website: http://www.fcc.gov/oet/rfsafety/dielectric.html

[14] BERENGER J.P.: 'A perfectly matched layer for the absorption of electromagnetic waves', *J. Comput. Phys.*, 1994, **114**, pp. 185–200

[15] NORTON K.A.: 'The physical reality of space and surface waves in the radiation field of radio antennas', *IRE Proc.*, 1937, **25**, (9), pp. 1192–1202

[16] BARLOW H.M.: 'Surface waves', *IRE Proc.*, 1958, **46**, (7), pp. 1413–1417

[17] MACLEAN T.S.M., WU Z.: 'Radio wave propagation over ground' (Springer, 1993)

[18] BELMONTE R., FAST S., SCHUSTER J.: 'A comparison of near earth propagation over layered media'. Proc. IEEE Military Communications Conf. (MILCOM), 2008, pp. 1–6

doi: 10.1049/iet-map.2008.0339